# VASCULAR NETWORK SEGMENTATION: AN UNSUPERVISED APPROACH

*Xavier Descombes*[1], *Franck Plouraboué*[2], *Abdelhakim El Boustani*[2,3], *Caroline Fonta*[4]
*Géraldine Le Duc*[5], *Raphael Serduc*[6], *Timm Weitkamp*[7] *

[1] I3S/INRIA/IBV, 2000 route des Lucioles, BP121, 06903 Sophia Antipolis Cedex, France
[2] IMFT UMR 5502 CNRS/INPT/UPS, av. du Pr. Camille Soula, 31400 Toulouse, France
[3] Ecole Nationale des Sciences Appliques de Tanger (ENSA), BP 1818, Tanger, Morocco
[4] CerCo UMR 5549, CNRS/Univ. P Sabatier, CHU Purpan Pavilllon Baudot, 31052 Toulouse cedex 03, France
[5] ESRF, 6 rue Jules Horowitz, BP220, 38043 Grenoble Cedex 9, France
[6] INSERM, U836, Univ. Joseph Fourier, Institut des Neurosciences, UMR-S836, Grenoble, F-38043, France
[7] Synchrotron Soleil, BP 48, 91192 Gif-sur-Yvette, France

## ABSTRACT

Micro-tomography produces high resolution images of biological structures such as vascular networks. In this paper, we present a new approach for segmenting vascular network into pathological and normal regions from considering their micro-vessel 3D structure only. We consider a partition of the volume obtained by a watershed algorithm based on the distance from the nearest vessel. Each territory is characterized by its volume and the local vascular density. The volume and density maps are first regularized by minimizing the total variation. Then, a new approach is proposed to segment the volume from the two previous restored images based on hypothesis testing. Results are presented on 3D micro-tomographic images of the brain micro-vascular network.

***Index Terms***— Segmentation, Total variation, Graph Cut, Hypothesis testing, micro-tomography, brain tumor

## 1. INTRODUCTION

High resolution micro-tomography provides an efficient imaging technique for the systematic 3D analysis of supracellular structures such as micro-vascular networks [1]. Since the diameters of most capillary vessels are distributed between 5 and 9 microns, micrometric spatial resolution is necessary for such a method to capture the entire vascular network, as for example for brain normal or pathological tissues [2]. At the millimeter scale, the number of vessels is very important, so that it is not reasonable to perform manually any vessel segmentation. It is thus necessary to develop automatic segmentation methods for a systematic, quantitative, reliable and differentiated investigation of normal and pathological networks. Such segmentation allows ultimately a detailed comparison between normal and pathological vessel networks with respect to their shape and spatial distribution as well as the determination of the angiogenic regions of a given tumor. A reliable automated segmentation would be of high interest because there is indeed a growing evidence in the recent literature that the maturation and maybe the normalization of tumoral vascular networks may be related to the observed resistance of the brain tumors to various treatments [3].

In this paper, we propose a segmentation method adapted to normal/tumorous vessel networks. This general segmentation scheme consists of data regularization leading to a first over-segmentation (see section 3) followed by a class merging algorithm based on hypothesis testing (see section 4). We thus avoid the tricky problem of likelihood modeling and associated parameters estimation or calibration. We apply this unsupervised segmentation scheme to a $3D$ partition obtained through the watershed computed on binary volumes composed of a background and a 3D network representing the vessels (see section 5).

## 2. MICRO-VASCULAR TERRITORIES

We start with X-ray tomography volumes binarized with an hysteresis thresholding. We consider the watershed obtained from the opposite distance map between each voxel and the nearest vessel, as proposed in [5]. Figure 2 shows the watershed partition obtained from the data given on figure 1. From this partition we introduce the notion of Local Vascular Territories (LVT) as follows:

**Definition 1** *A Local Vascular Territory (LVT) is a connected region corresponding to the catchment bassin associated with a vascular element. It can be obtained through the watershed computation on the opposite distance map from the vessels and is not connected to the sample border.*

*This research was supported by the ANR project "Micro-Réseaux", and the PEP II program from CNRS.

In the sequel, we propose an algorithm for grouping LVTs into global territories representing different tissues, such as sane or tumoral. Besides, we show that some properties of LVTs (volume, vessel density) are statistically significant for characterizing the tissues.

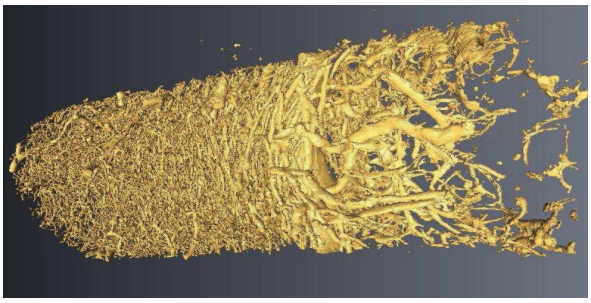

**Fig. 1**. Binarized vascular network

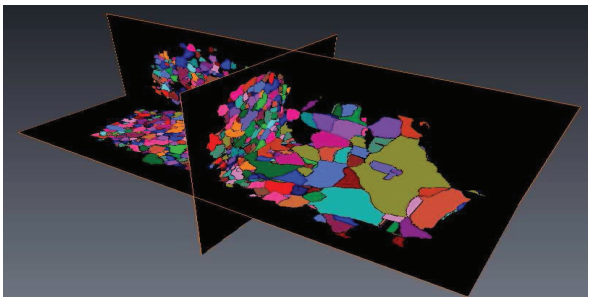

**Fig. 2**. Local vascular territories

## 3. TOTAL VARIATION MINIMIZATION

We consider two types of information for characterizing the LVT which are the territory volume and the vascular density (number of voxels belonging to vessels divided by the territory size in voxels). Each information is regularized by considering a Markov Random Field (MRF) modeling. We consider a graph $\mathcal{G}$ where the nodes $i$ correspond to the LVT which are not connected with the image border. We compute for each node the volume $v_i^{(0)}$ and the density $d_i^{(0)}$ of the corresponding LVT, and consider them as data. Edges are defined on adjacent LVT inducing a neighborhood relation $\sim$. As shown in [5], the log-log histogram of the territory sizes has a linear behavior. We consider for each node $i \in G$ a couple of variables consisting of the regularized density and log of the territory volume $(d_i, \log v_i)$. We obtain two maps corresponding to these two features for each LVT. To reduce the local variability of these maps we define a regularization process based on a Markov Random Field modeling [6]. Considering a Bayesian framework, we define the posteriors

$$P(X|Y) = \frac{P(Y|X)P(X)}{P(Y)} \propto P(Y|X)P(X), \qquad (1)$$

where $X$ represents the regularized map, $Y$ are the data. $P(Y|X)$ is the likelihood and $P(X)$ the prior. The goal is to smooth locally the variability of both the vessel density and the territory size. However, we want to preserve edges between the different tissus. To combine these two properties we propose to define priors minimizing the total variation, so that we have

$$P(X) = \frac{1}{Z} \exp\left[-\lambda \sum_{\{i,j\}:i\sim j} s_{i,j} \left|x_i - x_j\right|\right]. \qquad (2)$$

where $Z$ is the normalization constant.

Note that we weight each term by the area $s_{i,j}$ of the common face between LVTs $i$ and $j$, so that the influence of a neighbor territory depends on the area of their contact surface. The total weight of the sum of terms which involve a given node $i$ is thus equal to the total area of the corresponding territory borders. To prevent from over-regularizing large territories, while under-regularizing small ones, we consider the following data term

$$P(Y|X) = \frac{1}{Z'} \exp\left[-\sum_i S_i \left|x_i - y_i\right|\right] \qquad (3)$$

where $S_i = \sum_{j\sim i} s_{i,j}$ is the total surface of LVT $i$, $Z'$ is the normalizing constant. To regularize the density (resp. the volume) map we consider $x_i = d_i$ (resp. $x_i = \log v_i$) and $y_i = d_i^{(0)}$ (resp. $y_i = \log v_i^{(0)}$).

We perform the optimization with a graphcut algorithm, which has proved to outperform the simulated annealing algorithm in term of computational time. To address the proposed first order MRF in a multi-label context, we consider $\alpha$-expansion moves [7]. At each iteration, we propose for each node, either to keep the current value or to change it for a previously chosen one. This choice is made in order to minimize the energy. The different labels are then tested iteratively.

Figure 3 (resp. 4) shows an exemple of the obtained result for the volume (resp. density) regularization on one slice. We obtain segmented maps where the grey level represents two different variables issued from the LVT volumes and vascular densities respectively. We can notice that the spatial consistency has been largely improved as we can observe respectively two and three main regions on this slice. Each region is associated with a statistical distribution of respectively the LVT volumes and vessel densities. Note also that the algorithm depends on a single parameter $\lambda$, which has been fixed to 4 for all the database we consider. We have remarked that we obtain similar results for $\lambda$ between 3 and 10. Besides, the robustness with respect to $\lambda$ parameter will be again improved in the next step, consisting of volume and density maps fusion.

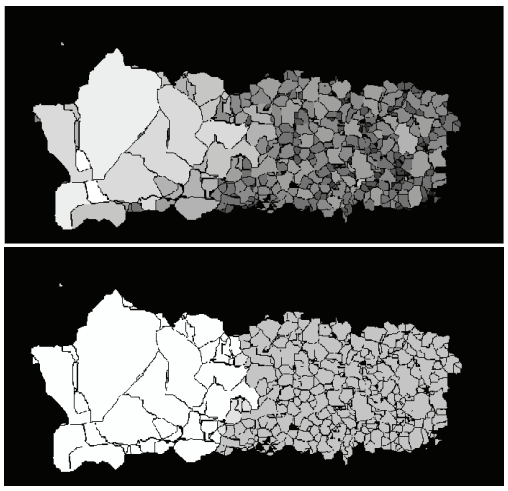

**Fig. 3**. Slice of the VLT volumes before (top) and after (bottom) regularization for $\lambda = 4$

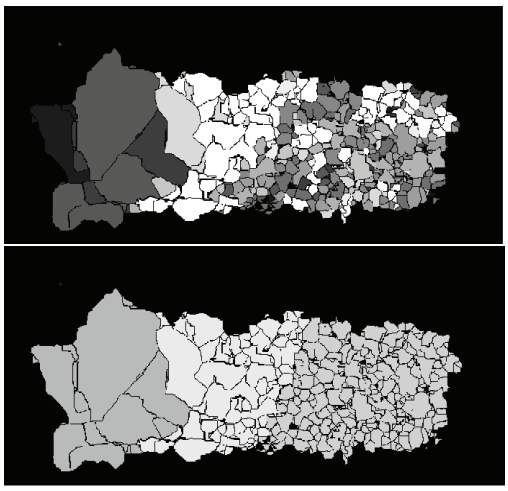

**Fig. 4**. Slice of the VLT vascular densities before (top) and after (bottom) regularization for $\lambda = 4$

## 4. HYPOTHESIS TESTING SEGMENTATION

We have obtained two regularized maps corresponding respectively to the volumes of LVT and their vascular density. To merge these informations we propose a fusion scheme resulting in a single segmentation of the whole volume into several classes, whose number is unknown. Let us denote by $L_V$ (resp. $L_D$) the set of values taken by the different nodes on the regularized log-volume (resp. density). To initialize the segmentation, we consider all non empty classes in $L_S \times L_D$. We denote by $c_i, i \in \{1, \ldots, N\}$ these classes. We then propose to merge classes which are not statistically significantly different. Each class is characterized by the distributions of two variables, the log-volume and the density, which are correlated. The merging criterion is then based on a MANOVA (Multivariate ANalysis Of Variance) test. MANOVA is based on variance analysis and can be seen as an extension of ANOVA in case of dependant variables. We have defined an algorithm which iteratively merges in parrallel the closest couple of classes until each remaining class is statistically significantly different from others (see algorithm 1). This algorithm, only based on class statistics, does not require the definition of class likelihood and thus avoids estimating or calibrating some parameters.

## 5. RESULTS

We consider images of vessels of the cerebral cortex obtained from synchrotron tomography imaging at the European Synchrotron Radiation Facility (ESRF) [1, 4]. They come from rat brain implanted with 9L gliosarcoma cells. The resolution is 1.4 micron and a dataset represents about $8\mathrm{mm}^3$. The reconstructed image is first binarized using hysteresis thresholding and mathematical morphological open/closure procedures. Some results are shown on figure 5 where clusters correspond to tumor (red), necrosis (blue), periphery (yellow) and sane (green) tissues. The computation of the LVT volumes and densities is given in table 1 and summarized on figure 6. Although we can notice some variability between samples, due to individuals but also to the different delays between the tumor irradiation and the animal euthanasia, we can see a clear difference between the tumor class (high volumes and high vascular densities), the sane class (low volumes and low densities) and the intermediate class corresponding to the periphery of the tumor where the vessel density increases, due to angiogenesis, while the volume does not significanlty evolve.

## 6. CONCLUSION

We have proposed a new two-step unsupervised segmentation scheme consisting of a regularization algorithm minimizing the total variation followed by a class merging based on statistical hypothesis testing. This approach has been applied to segment micro-vascular networks. The different territories have been interpreted a posteriori by biologists as sane, tumor, interface and necrotic tissues. The different classes are characterized by specific vascular densities and LVT volumes. The proposed approach could be applied to any segmentation problem, including grey scale or color images. The main idea is first to regularize the data to obtain an initial segmentation, and then to merge neighbor classes which are not statistically significantly different. For our application, the next step will consist in modelling the different vascular networks. We aim at characterizing the vascular network topology changes that occur during the transitions between the different classes.

N = number of classes (classes which contain less than 2 VLT are excluded),
$\forall\{i,j\} \in \{1,\ldots,N\} \times \{1,\ldots,N\}$ such that $i \neq j$ set $p(i,j) = 1$,
**repeat**
  **for** Every couple $(i,j), i \neq j$ of the current classes **do**
    Compute $p(i,j)$ the p-value corresponding to the MANOVA test between population $i$ and $j$ and set the label VALID for each class $i$
  **end for**
  **repeat**
    search $(I,J) = \arg\min_{(i,j):i,jVALID} p(i,j)$
    merge classes $I$ and $J$ ; set $I$ and $J$ to NONVALID ; $N \leftarrow N-1$
  **until** There exits a couple $(i,j)$ of two VALID classes such that $p(i,j) \leq 0.05$
**until** $\forall\{i,j\} \in \{1,\ldots,N\} \times \{1,\ldots,N\}$ such that $i \neq j$, $p(i,j) > 0.05$

**Algorithme 1:** Classes merging by hypothesis testing

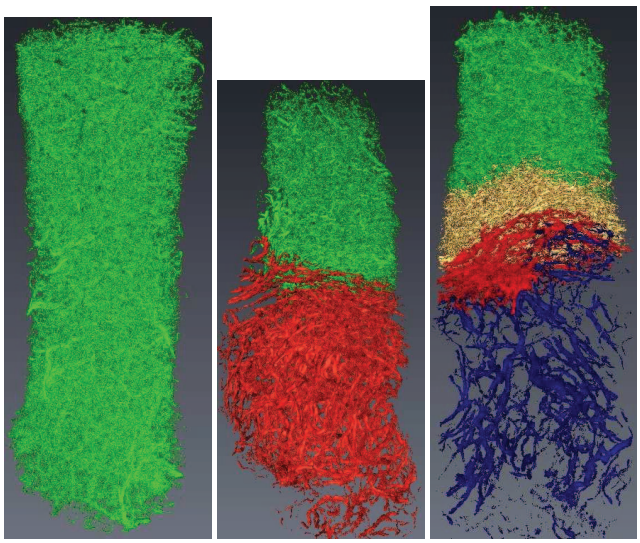

**Fig. 5**. Examples of segmentation: tumor (red), necrosis (blue), tumor periphery (yellow) and sane (green)

## 7. REFERENCES


[1] F. Plouraboué, P Cloetens, C. Fonta, A. Steyer, F. Lauwers and J. Marc-Vergnes. *High resolution x-ray imaging of vascular networks*. J. Microscopy, 215(2):139-148, 2004.

[2] L. Risser, F. Plouraboué, A. Steyer, P. Cloetens, G. Le Duc and C. Fonta. *From homogeneous to fractal normal and tumorous micro-vascular networks in the brain*. J. Cer. Blood Flow and Metab., 27:293-303, 2007.


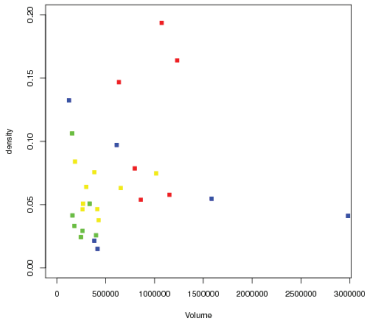


**Fig. 6**. Vessel density versus volume for tumor (red), necrosis (blue), tumor periphery (yellow) and sane (green) territories

| | | | | | | |
|---|---|---|---|---|---|---|
| D+2 | S | $3.3 \times 10^5$ | 0.05 | T | $6.4 \times 10^5$ | 0.15 |
| | P | $4.1 \times 10^5$ | 0.05 | N | $3.1 \times 10^5$ | 0.10 |
| D+2 | S | $2.5 \times 10^5$ | 0.02 | T | $1.2 \times 10^6$ | 0.16 |
| | P | $3.0 \times 10^5$ | 0.06 | | | |
| D+7 | S | $4.0 \times 10^5$ | 0.03 | T | $8.0 \times 10^5$ | 0.08 |
| | P | $4.3 \times 10^5$ | 0.04 | N | $3.8 \times 10^5$ | 0.02 |
| | N | $4.2 \times 10^6$ | 0.01 | | | |
| D+7 | T | $1.1 \times 10^6$ | 0.19 | P | $1.0 \times 10^6$ | 0.07 |
| D+14 | S | $2.6 \times 10^5$ | 0.03 | T | $8.6 \times 10^5$ | 0.05 |
| | P | $2.7 \times 10^5$ | 0.05 | N | $3.0 \times 10^6$ | 0.04 |
| D+14 | S | $1.8 \times 10^5$ | 0.03 | T | $1.2 \times 10^6$ | 0.06 |
| | P | $2.6 \times 10^5$ | 0.05 | N | $1.6 \times 10^6$ | 0.05 |
| D+14 | S | $1.6 \times 10^5$ | 0.04 | | | |

**Table 1**. Samples (delay in days between irradiation and euthanasia), Territory classification (Sane, Tumor, Periphery and Necrosis), Volume in $\mu m^3$ and vascular density in relative volume


[3] R.K. Jain et al. *Angiogenesis in brain tumours*. Nat Rev Neurosci, 8(8): p. 610-22, 2007.

[4] T. Weitkamp, P. Tafforeau, E. Boller, P. Cloetens, J.-P. Valade, P. Bernard, F. Peyrin, W. Ludwig, L. Helfen, and J. Baruchel. *Status and evolution of the ESRF beamline ID19*. In proc. AIP, 1221:33-38, 2010.

[5] X. Descombes, F. Plouraboué, H. El Boustani, C. Fonta, G. Le Duc, R. Serduc and T. Weitkamp. *Brain tumor vascular network segmentation from micro-tomography* In Proc. ISBI, 2011.

[6] D. Geman and S. Geman. *S*tochastic Relaxation, Gibbs Distributions, and the Bayesian Restoration of images IEEE T. on PAMI, 6(6):721-741, 1984.

[7] Y. Boykov, O. Veksler and R. Zabih. *Fast Approximate Energy Minimization via Graph Cuts* IEEE T. on PAMI, 23(11):1222-1239, 2001.